

## Review

# The role of deep learning in myocardial perfusion imaging for diagnosis and prognosis: A systematic review

Xueping Hu,<sup>1,2,5</sup> Han Zhang,<sup>1,2,5</sup> Federico Caobelli,<sup>3,5</sup> Yan Huang,<sup>1,2,5</sup> Yuchen Li,<sup>1,2</sup> Jiajia Zhang,<sup>1,2</sup> Kuangyu Shi,<sup>3,4</sup> and Fei Yu<sup>1,2,\*</sup>

<sup>1</sup>Department of Nuclear Medicine, Shanghai Tenth People's Hospital, Tongji University School of Medicine, Shanghai, China

<sup>2</sup>Institute of Nuclear Medicine, Tongji University School of Medicine, Shanghai, China

<sup>3</sup>Department of Nuclear Medicine, Inselspital, Bern University Hospital, University of Bern, Bern, Switzerland

<sup>4</sup>Computer Aided Medical Procedures and Augmented Reality, Institute of Informatics I16, Technical University of Munich, Munich, Germany

<sup>5</sup>These authors contributed equally

\*Correspondence: [yufei\\_021@163.com](mailto:yufei_021@163.com)

<https://doi.org/10.1016/j.isci.2024.111374>

## SUMMARY

The development of state-of-the-art algorithms for computer visualization has led to a growing interest in applying deep learning (DL) techniques to the field of medical imaging. DL-based algorithms have been extensively utilized in various aspects of cardiovascular imaging, and one notable area of focus is single-photon emission computed tomography (SPECT) myocardial perfusion imaging (MPI), which is regarded as the gold standard for non-invasive diagnosis of myocardial ischemia. However, due to the complex decision-making process of DL based on convolutional neural networks (CNNs), the explainability of DL results has become a significant area of research, particularly in the field of medical imaging. To better harness the potential of DL and to be well prepared for the ongoing DL revolution in nuclear imaging, this review aims to summarize the recent applications of DL in MPI, with a specific emphasis on the methods in explainable DL for the diagnosis and prognosis of MPI. Furthermore, the challenges and potential directions for future research are also discussed.

## INTRODUCTION

Ischemic heart disease (IHD) accounts for the largest proportion of cardiovascular disease globally and has the highest age-standardized disability-adjusted life years at 2,275.9 per 100,000 people.<sup>1</sup> Given the prevalence and impact of IHD, early diagnosis and effective management strategies are crucial for improving patient outcomes and alleviating the burden on healthcare economies.<sup>2</sup> Single-photon emission computed tomography (SPECT) myocardial perfusion imaging (MPI) is considered the gold standard for non-invasive diagnosis of myocardial ischemia, and it has shown potential for predicting outcomes in patients with IHD.<sup>3</sup> However, the semi-quantitative limitations of MPI measurements and the presence of image artifacts, such as liver interference, have contributed to a decrease in the diagnostic accuracy of MPI, particularly for detecting balanced and subtle myocardial ischemia. Additionally, perfusion positron emission tomography (PET) MPI is currently used more for scientific research as it is limited by its high price and short nuclide half-life.

Deep learning (DL) was initially introduced by Hinton et al.<sup>4</sup> in 2006, showcasing its ability to automatically learn complex and high-dimensional information through the utilization of multi-layer non-linear convolutional neural networks (CNNs). This

breakthrough opened up new avenues in the field of medical imaging and was initially applied in radiomics, where it showed excellent performance especially in the detection of tumor heterogeneity, and was later widely used in radiology, including image reconstruction, accurate segmentation, and assisted diagnosis.<sup>5</sup> Currently, DL has shown a greater potential in improving MPI diagnosis and prognosis.<sup>6</sup> In order to help clinicians to better understand and apply the results of DL and to be prepared for the ongoing DL revolution in cardiovascular imaging, this review summarizes and discusses the main clinical applications of DL in MPI, including the diagnosis of myocardial ischemia, prognosis prediction, and image attenuation correction (AC). Moreover, the challenges and potential directions of DL for future MPI from a clinical perspective are discussed.

## SEARCH STRATEGY

In conducting the systematic literature review, a three-step process was employed, consisting of research question identification, literature search, and review analysis. Initially, the research question was established, and a review protocol was developed that specified the database sources and search terms. In the second step, the literature was collected and filtered in accordance with the review protocol. Finally, the selected literature



was analyzed to extract and synthesize the data necessary to address the research question, and the results of the review were documented.

### Research questions

The primary aim of this review is to evaluate the diagnostic and prognostic applications of DL in MPI for ischemic heart disease. Additionally, the review explores the indicators involved and their applications. This synthesis of current studies serves as a foundation for further investigation into future challenges and potential research directions. Consequently, we formulated the following three research questions.

- (1) What specific DL neural network or model was employed?
- (2) Which MPI features and clinical variables were integrated into the DL models?
- (3) How can the results generated by DL be utilized to diagnose myocardial ischemia and predict prognosis in MPI?

In our review of the literature, we adopted a focused approach, ensuring that each article addressed the aforementioned questions. We present a synthesis of the collected data to provide a comprehensive overview of the findings.

### Search sources and terms

Three prominent scientific databases PubMed, Scopus, and Google Scholar, as well as additional methods, were utilized for data extraction. The search strategy incorporated medical subject headings (MeSH) and text terms in the following categories: (1) “deep learning,” “deep network,” “artificial intelligence,” “convolutional neural network,” and “artificial neural network” related to research methodology; (2) “nuclear medicine,” “SPECT,” and “myocardial perfusion imaging” pertaining to the medical field; (3) “coronary artery disease,” “cardiovascular,” “myocardial,” “heart,” and “cardiac” concerning the diseases studied. Original research literature examining the diagnostic and prognostic applications of DL in MPI was screened.

Search String in PubMed and Google Scholar: ((deep learning) OR (deep network) OR (artificial intelligence) OR (convolutional neural network) OR (artificial neural network)) AND ((SPECT) OR (myocardial perfusion imaging) OR (nuclear medicine)) AND ((coronary artery disease) OR (cardiovascular) OR (myocardial) OR (heart) OR (cardiac)).

Search String in Scopus: (TITLE-ABS-KEY (“deep learning”) OR (“deep network”) OR (“artificial intelligence”) OR (“convolutional neural network”) OR (“artificial neural network”)) AND TITLE-ABS-KEY (“SPECT nuclear medicine”) OR (“myocardial perfusion imaging”) OR (“nuclear medicine”)) AND TITLE-ABS-KEY (“coronary artery disease”) OR (“myocardial”) OR (“cardiovascular”) OR (“cardiac”) OR (“heart”)).

### Eligibility criteria

This study focused on the application of DL for the diagnosis and prognostic prediction of myocardial ischemia in MPI. Following the completion of title checks, a set of inclusion and exclusion criteria was applied to all sections of the abstract and full text during the review process. Papers that met the following criteria

were deemed eligible for review: (1) published in peer-reviewed journals, (2) utilizing DL as the primary research method, (3) employing myocardial perfusion images obtained from SPECT as the primary research device, (4) aiming to enhance diagnostic or prognostic efficacy in patients with IHD, (5) written in English, and (6) published between 2017 and July 2024 to ensure the inclusion of the most recent data. Literature that failed to provide a clear number of cases, as well as conference proceedings and expert opinions, was excluded.

A secondary search was conducted by manually reviewing the literature sections of relevant studies, which were limited to those with available full texts. For studies lacking full texts, authors were contacted; however, if the authors did not respond or were unable to provide the full texts, these studies were excluded from consideration. Search queries were constructed to incorporate the aforementioned terms in the titles of the articles.

### Literature collection

Literature searches were conducted by employing specific search strings for each database, resulting in numerous publications responding to these queries. Search results for each database were evaluated against established eligibility criteria. During the initial screening, literature published prior to 2017 and duplicates were excluded. Each article was assessed based on its title and abstract to determine eligibility for inclusion or rejection, leading to a reduction in the number of documents to 179. The subsequent screening phase involved a thorough review of the text and the availability of full-text content, ultimately leading to the selection of 26 studies for inclusion in this literature review. This systematic review was performed in accordance with the guidelines established by PRISMA (Preferred Reporting Items for Systematic Reviews and Meta-Analyses).<sup>7</sup> The QUADAS-2 tool is used to measure the risk of bias in the conducted studies. The entire process is illustrated in [Figures 1 and 2](#).

### DL DIAGNOSTIC EVALUATION FOR MYOCARDIAL ISCHEMIA

DL models can capture and learn intricate patterns within MPI images, facilitating the identification of myocardial abnormalities. Most models were trained with polar maps and compared with total perfusion deficit (TPD), which is the degree of myocardial ischemia as a percentage of left ventricular myocardium.<sup>8</sup> [Table 1](#) summarizes the application of DL in MPI diagnosis.

### DL diagnostic models

The DL model with integrated polar maps is superior to conventional TPD for the diagnosis of myocardial ischemia. Betancur et al.<sup>17</sup> trained DL models with stress-only raw and blackout polar maps to predict the probability of obstructive stenosis from a multi-center registry. And the clinically relevant variable gender<sup>11</sup> was included in the model. The area under the curve (AUC) of the DL outperformed TPD (per patient: 0.80 vs. 0.78; per vessel: 0.76 vs. 0.73,  $p < 0.01$ ). Clinicians commonly combine upright and supine images to improve the diagnostic accuracy of MPI. Later, Betancur et al.<sup>13</sup> used the same DL network to combine

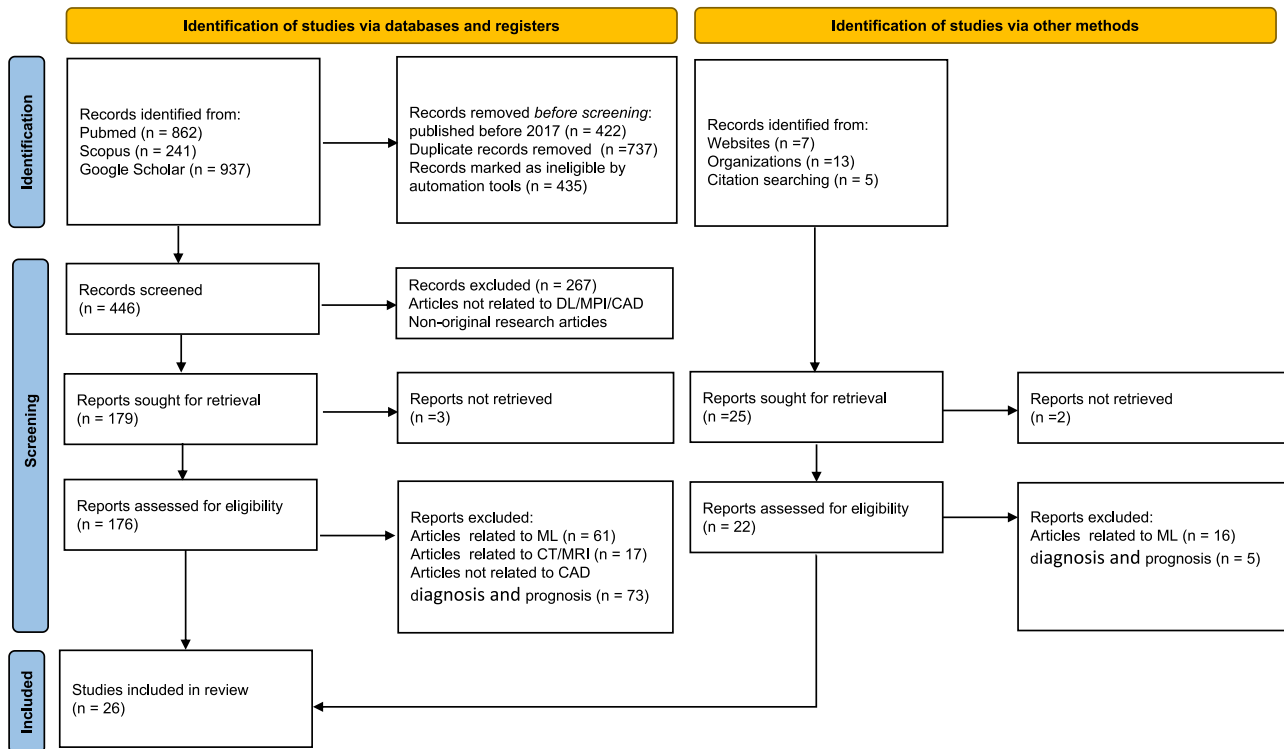


Figure 1. Search strategy and eligibility criteria

upright and supine stress-only polar maps to predict obstructive stenosis. A similar result was achieved, as the DL model-predicted obstructive disease outperformed combined TPD (AUC per patient: 0.81 vs. 0.78; per vessel: 0.77 vs. 0.73,  $p < 0.001$ ).

Besides polar maps being used for DL diagnostic models, the cardiac axial images have also been used. MPI cardiac axial images include short-axis (SA), horizontal long-axis (HLA), and vertical long-axis (VLA). And the polar map is generated by the projection of a multilayer SA images onto a two-dimensional plane. Subsequently, Liu et al.<sup>18</sup> trained the ResNet-34 network with stress-only MPI cardiac axial images from a large sample study enrolling 37,243 patients to identify myocardial ischemia. In addition, 6 clinically relevant clinical characteristics (including gender, body mass index, length, stress type, radiotracer and AC) were incorporated into the model. The results showed that the DL model identified myocardial perfusion abnormalities outperformed TPD (AUC 0.87 vs. 0.84,  $p < 0.01$ ). Furthermore, the study referred that DL networks with cardiac axial maps performed slightly better than that with polar maps, which may be related to the semi-quantitative measures of the blackout polar maps.

Traditionally, stress MPI images have been assumed to provide more valuable information about myocardial perfusion compared to rest images. However, studies suggested that patients with normal stress MPI results can still exhibit myocardial ischemia, which may be attributed to abnormalities in rest myocardial blood perfusion.<sup>14</sup> Simultaneous evaluation of both images may improve the detection of myocardial ischemia. Berkaya et al.<sup>19</sup> trained both DL-based and knowledge-based clas-

sification models with rest and stress MPI cardiac axial images to identify myocardial ischemia. The results indicated that those two models respectively achieved 94% and 93% diagnostic accuracy, compared to two experts' diagnosis. Later, Wang et al.<sup>9</sup> trained ResNet18 model with rest and stress MPI cardiac axial images to identify myocardial ischemia. The results presented the model diagnosis of myocardial perfusion abnormalities with AUC above 0.95. Recently, Papandrianos et al.<sup>16</sup> trained RGB-CNN model with rest and stress MPI images to identify myocardial perfusion ischemia and infarction. The results suggested that the model diagnostic accuracy was 91.86% compared to the physician's diagnosis.

### Explainable DL diagnostic models

Since the decision-making process of DL networks is sophisticated and obscure, DL is often considered a "black box" and its explainability is crucial to broaden its clinical applications. Otaki et al.<sup>10</sup> trained a coronary artery disease (CAD)-DL model to diagnose obstructive CAD using 3 polar maps, which included stress myocardial perfusion, motion, and thickening maps. Additionally, 3 clinically relevant variables (including LV volume, age, and sex) were included in the model. The findings revealed that CAD-DL diagnosis of myocardial ischemia outperformed both TPD and physician diagnosis (AUC 0.83 vs. 0.78 vs. 0.71,  $p < 0.001$ ). Remarkably, the investigators generated a "CAD attention map" based on gradient-weighted class activation mapping (Grad-CAM), which can visualize the underlying principles of CAD-DL prediction. The principle of Grad-CAM involves calculating the weights of each channel by performing global

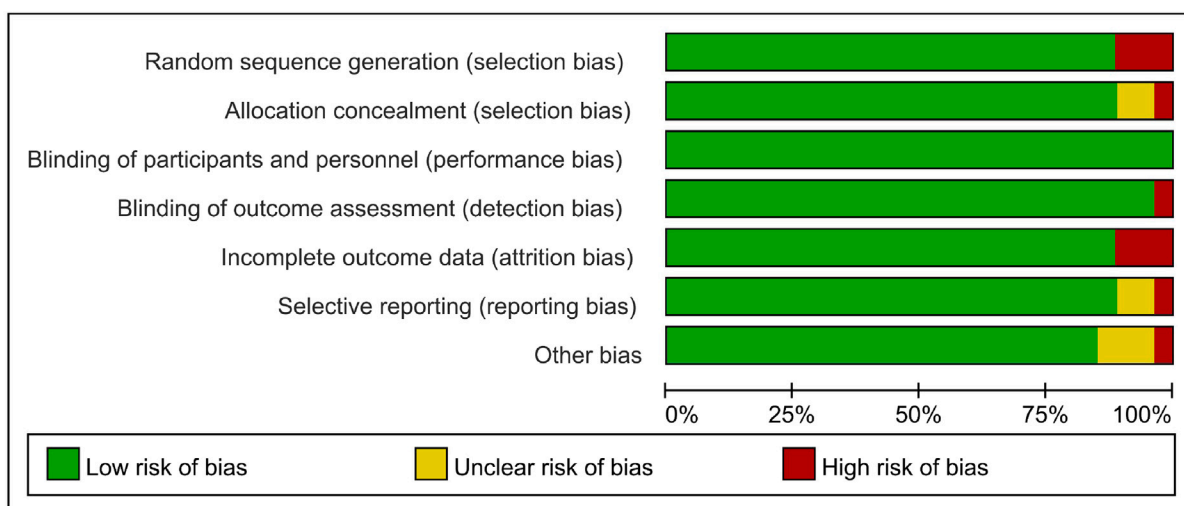
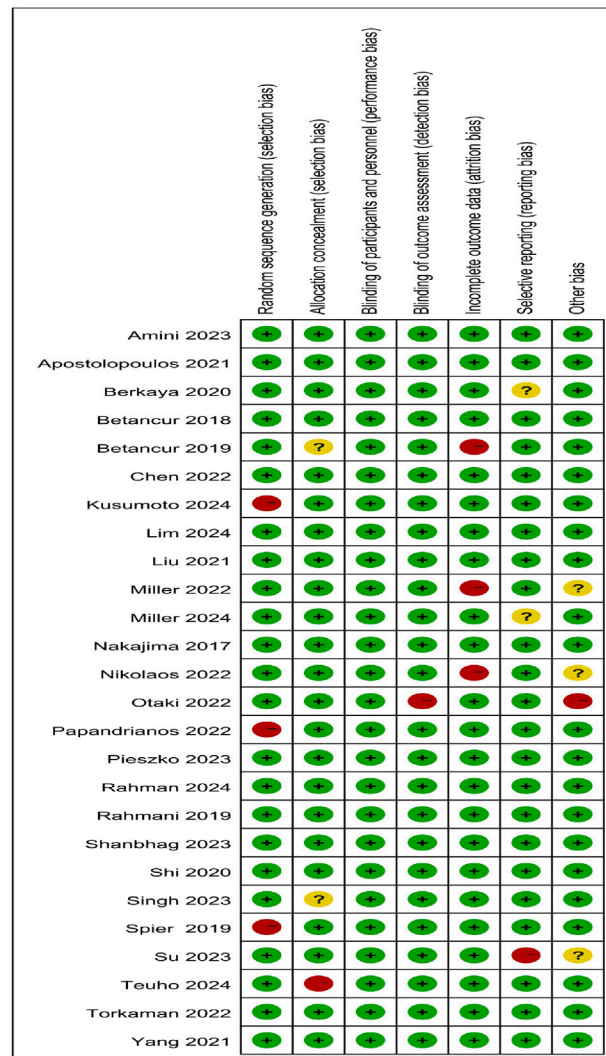


**Figure 2. The risk of bias of the conducted studies was measured using the QUADAS-2 tool**

The risk of bias shown in the figure above indicates the number and percentage of studies with a high (red), medium (yellow), and low (green) risk of bias for each of the four groups QUADAS-2 tool.

**Table 1. Clinical applications of DL in MPI diagnosis**

Authors	Year	Total N	Site(s)	DL	Input variables	Comparison	Evaluation
Nathalia Spier et al.	2019	946	1	GCNNs	rest and stress polar maps	human observer	agreement 83.1%
Mehdi Amini et al.	2023	395	1	classification	rest and stress MPI radiomics features, clinical features	no CAD vs. CAD, and low-risk/high-risk CAD	AUC 0.61 vs. 0.79
Ting-Yi Su et al.	2023	694	1	3D-CNN	resting-state images	SSS, SDS, and SRS	accuracy 87.08% sensitivity 86.49% specificity 87.41%
Ioannis D. Apostolopoulos et al.	2021	566	1	CNNs	AC and NAC polar maps, clinical data	medical expert	accuracy 79.15% sensitivity 89.17% specificity 71.20%
Papandrianos et al. <sup>9</sup>	2022	842	1	RGB-CNN	SA, HLA, and VLA images	VGG-16 and DenseNet-121 model	accuracy 88.54% and 86.11%
R Rahmani et al.	2019	923	1	ANN	stress and rest polar plots, age, gender, and the number of risk factors	result of angiography, obstructive CAD, and Gensini score	accuracy 92.9% vs. 85.7% vs. 92.9%
Papandrianos et al. <sup>9</sup>	2022	314	1	RGB-CNN, VGG-16	stress and rest polar maps in AC and NAC format	TPD	accuracy 92.07% vs. 95.83%
Betancur et al. <sup>8</sup>	2018	1,638	9	Deep CNN	raw and quantitative polar maps	TPD	AUC per patient 0.80 vs. 0.78 per vessel 0.76 vs. 0.73
Otaki et al. <sup>10</sup>	2022	3,578	5	CNNs	stress myocardial perfusion, wall motion, and wall thickening maps; left ventricular volumes, age, and sex	TPD and physician diagnosis	AUC 0.84 vs. 0.78 vs. 0.71
Betancur et al. <sup>11</sup>	2019	1,160	4	Deep CNN	upright and supine polar MPI maps	combined TPD	AUC per patient 0.81 vs. 0.78 per vessel 0.77 vs. 0.73
Miller et al. <sup>12</sup>	2022	240	1	Deep CNN	stress myocardial perfusion, wall motion, and wall thickening maps; left ventricular volumes, age, and sex	physician interpretation without CAD-DL and TPD	AUC 0.78 vs. 0.75 vs. 0.72
Kenichi Nakajima et al.	2017	1,001	12	ANN	stress, rest, and difference features	SSS, SDS, and SRS	AUC 0.92 vs. 0.82 SDS 0.90 vs 0.75 SRS 0.97 vs 0.91
Liu et al. <sup>13</sup>	2021	37,243	1	Deep CNN	stress-only circumferential count profile maps, gender, BMI, length, stress type, radio tracer, and the AC option	quantitative defect size (DS)	AUC 0.87 vs. 0.84
Berkaya et al. <sup>14</sup>	2020	192	1	DNNs	SA, HLA, and VLA slices	two expert readers	accuracy 94% sensitivity 88% specificity 100%
Teuho et al. <sup>15</sup>	2024	138	1	Deep CNN	PET-CT, CTA, and clinical data	ICA	AUC 0.85
Kusumoto et al. <sup>16</sup>	2024	5,443	1	3D-CNN	SA, HLA, and VLA images; age and sex	medical expert	accuracy 88%



## Clinical Deployment of Explainable Artificial Intelligence

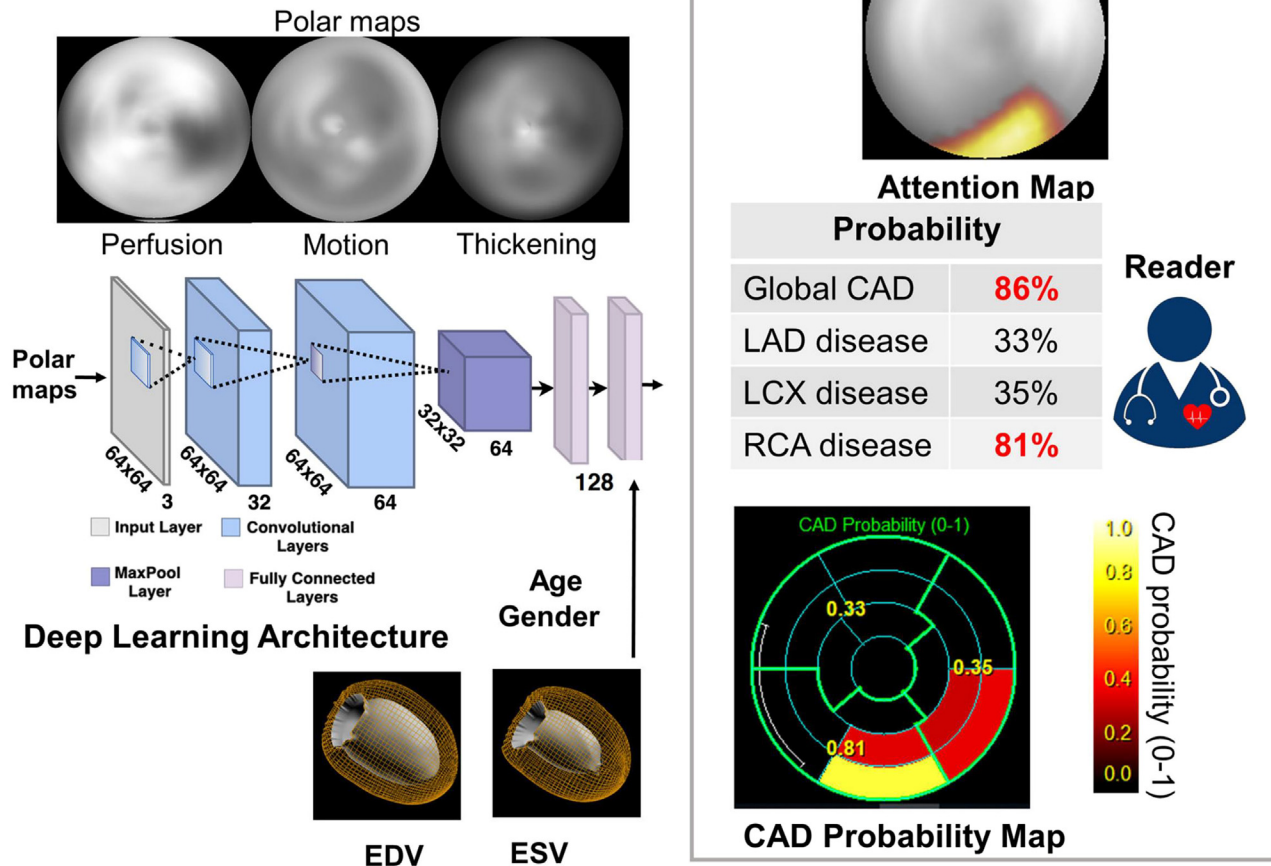


**Figure 3.** Otaki et al. trained a CAD-DL model: the raw myocardial perfusion, wall motion, and thickening images are input to the deep learning model “CAD-DL”

Remarkably, the investigators generated a “CAD probability map” based on gradient-weighted class activation mapping (Grad-CAM). For example, the CAD probability map in the figure indicates a high likelihood of CAD, particularly in the inferior and proximal lateral walls, which contribute to the prediction. This finding suggests a significant probability of obstruction in the right coronary artery, potentially with a gyratory branch.

average pooling on the gradients of the final convolutional layer. These weights are then used to weight the feature maps, resulting in the generation of a class activation map. This technique effectively visualizes which parts of the deep network contribute most significantly to the prediction results, thereby enhancing the explainability and visual clarity of the decision-making process within neural networks. The information in the CAD attention map is used to identify the corresponding segments and classify the probability of obstructive CAD, which is displayed as a “CAD probability map.” By visualizing the regions and probability of obstructive CAD, explainable DL assists the physician in assessing the relationship between the CAD-DL outcomes and the images. The researchers used attention maps to accentuate the left ventricular region, which aided the physician’s prediction. The entire process is illustrated in Figure 3.

DL has high independent diagnostic accuracy for obstructive CAD, but its impact on physician diagnosis is unclear. Miller

et al.<sup>12</sup> assessed whether obtaining explainable DL outcomes improved physician diagnosis based on the previous CAD-DL model. And it suggested that physicians with CAD-DL had a higher diagnostic accuracy compared to both physicians without CAD-DL and stress TPD (AUC 0.78 vs. 0.75 vs. 0.72,  $p < 0.001$ ). This suggests that DL has the potential to aid clinicians in their decision-making process. Furthermore, since the CAD-DL training cohort is at high risk of myocardial infarction (MI), disease probability may be overestimated owing to selection bias. Consequently, Miller et al.<sup>20</sup> evaluated different populations to train DL models to improve the accurate estimation of disease probability. The researchers approached a more real-life probability of disease by adding patients with a low likelihood of CAD (LLK) to the training cohort of the CAD-DL model. The findings indicated that the diagnostic performance of the model with LLK patients outperformed TPD (AUC 0.93 vs. 0.90,  $p < 0.01$ ), especially in female patients.

**Table 2. Clinical applications of DL in MPI prognosis**

Authors	Year	Total N	Site(s)	AI method	Input variables	Predicted outcome	Comparison	Evaluation
Singh et al. <sup>24</sup>	2023	20,401	5	HARD-MACE-DL	perfusion, motion, thickening, phase amplitude, and phase angle polar maps; age, sex, and cardiac volumes	all-cause mortality or non-fatal MI	logistic regression, stress TPD, and ischemic TPD	AUC 0.73 vs. 0.70 vs. 0.65 vs. 0.63
Pieszko et al. <sup>25</sup>	2023	20,418	5	DL	5 SPECT polar maps and 15 clinical features	all-cause death, ACS, revascularization	MACEs	AUC 0.76 vs. 0.78

In the inevitable future of multimodal image analysis, especially for cardiac imaging, the integration of anatomical and functional cardiac imaging will be beneficial for future clinician research. Recently, Teuvo et al.<sup>15</sup> applied the DL technique, integrating <sup>15</sup>O–H<sub>2</sub>O perfusion PET computed tomography (PET/CT) and coronary CT angiography (CTA) imaging, as well as clinical variables to detect myocardial ischemia. In addition, the DL model was applied to Grad-CAM and Shapley additive explanations (SHAP), which highlight the variables that contribute most to prediction, providing a basis for subjective application of results by clinicians. Overall, this study provides further evidence that multimodal AI can increase confidence in myocardial perfusion image analysis. It is worth noting that as multimodal AI approaches become more complex and integrate wider arrays of data, DL models will need to utilize sophisticated methods to measure the accuracy of the inputs and consider the time it takes to merge the inputs.

In practical clinical diagnosis of IHD, the characterization and localization of myocardial ischemia are crucial. The location of myocardial ischemia identified through MPI corresponds to the stenosis in the relevant coronary artery branch. To enhance clinicians' efficiency in utilizing this information, it is essential that the localization of myocardial ischemia is explainable, especially considering the black-box nature of DL models. Grad-CAM addresses this challenge by visualizing which parts of the DL model contribute to the prediction results. Furthermore, given the heterogeneity among patients, it is vital for clinical practice to incorporate demographic and medical history features—such as gender, age, and family history of coronary heart disease—into the diagnostic process. This integration enables a more nuanced understanding of how each feature influences model predictions, which can be assessed using SHAP values for each variable. By combining Grad-CAM with SHAP values, clinicians can perform individualized diagnoses of myocardial ischemia. This approach allows for a comprehensive analysis that integrates both the localization of myocardial ischemia and relevant clinical features, ultimately improving diagnostic accuracy.

### EXPLAINABLE DL PROGNOSTIC MODELS

In clinical practice, cardiovascular risk stratification is typically conducted using visual assessment and quantitative analysis of MPI. However, it is important to recognize that relying on these two assessments may overlook other clinical risk factors.<sup>21,22</sup> DL

has the potential to revolutionize the prognosis of MPI by integrating MPI images with prognostic variables to provide accurate probabilities of adverse cardiovascular events.<sup>23</sup> This innovative approach is expected to assist physicians in stratifying the management and delivering precise treatment to patients with IHD, ultimately reducing the incidence of adverse prognoses. Table 2 lists the applications of DL in MPI prognosis.

MPI has been proven to have prognostic value in predicting major adverse cardiovascular events (MACEs), but making accurate and individualized predictions is challenging. Singh et al.<sup>24</sup> trained an interpretable DL model (HARD-MACES-DL) to predict death and non-fatal MI using 5 polar maps, which include stress myocardial perfusion, motion, thickening, as well as phase amplitude and angle. Gender, age, and heart volume were also incorporated in the model. The predictive performance of the model outperformed stress TPD and ischemic TPD (AUC 0.73 vs. 0.65 vs. 0.63,  $p < 0.01$ ). The researchers used attention maps to accentuate the left ventricular region, which aided the physician's prediction. To quantify the weight of the input polar maps, SHAP values assign predicted significance values to each feature. SHAP is a model interpretation method grounded in game theory. It assigns an explanatory score to each feature by quantifying its contribution to the model's predicted outcome. This approach not only aids in understanding the rationale behind the model's predictions but also offers an intuitive explanation of the predicted results. These methods promote explainable outcomes, identifying important regions of imaging and the significance of features to be more fully assessed by physicians. The entire process is illustrated in Figure 4.

DL can make accurate predictions individually; however, it is more challenging to personalize predictions for specific event types with temporal dependencies. Recently, Pieszko et al.<sup>25</sup> trained a DL model to predict the time-specific risk of all-cause mortality, acute coronary syndrome (ACS), and revascularization. It incorporated the same 5 polar maps and additional 15 clinical features from 20,418 patients. The findings indicated the best model for predicting ACS and all-cause with AUC values of 0.76 and 0.78 ( $p < 0.001$ ), respectively. What's more, the waterfall charts generated from the SHAP values were used to visually explain the clinical variables that individualize the risk of specific events over time. It may enable physicians to achieve precision medicine through personalized treatment and preventive measures, which helps physicians and patients make decisions together.

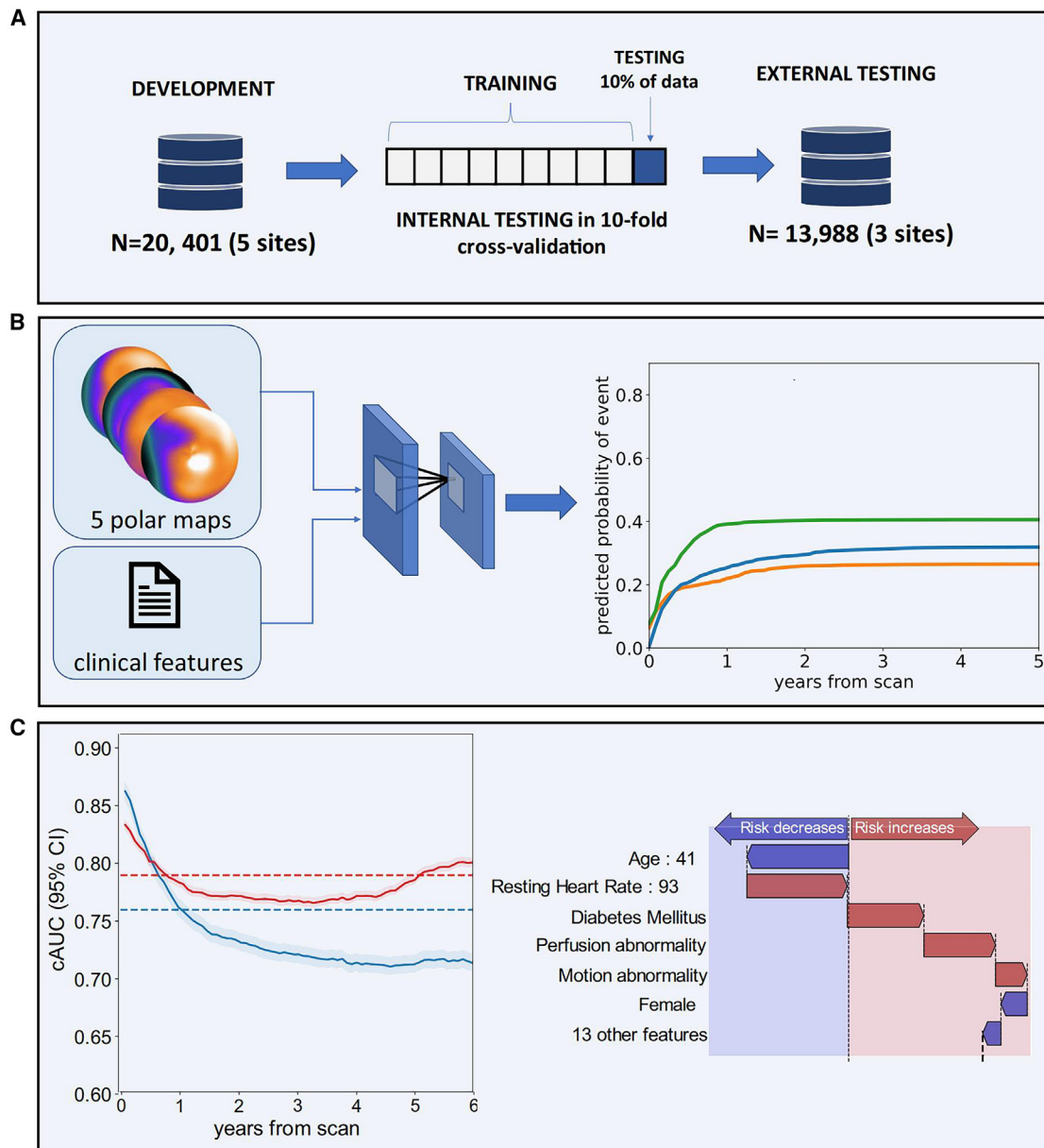


**Figure 4. Pieszko et al. trained a DL model: deep learning enabled time-to-event outcome prediction after cardiac imaging – Study overview**

In this case, (C) illustrates the application of SHAP diagrams. The performance of the model (left) was analyzed using the cumulative dynamic cAUC. (A), (B), and (C) in the upper left corner of the image represent the serial numbers of the figure. Red lines represent time-to-event models, while blue lines indicate perfusion abnormalities. The interpretation of predictions is visualized as a waterfall plot, with blue arrows denoting features that reduce risk and red arrows indicating features that increase risk (right). Abbreviations used in this context include ACS, AUC, TPD, PCI (percutaneous coronary intervention), and CI (confidence interval).

Factors influencing prognosis, along with the effects of adjusting for various variables, have gained significant attention in clinical practice when analyzing outcomes for patients with IHD. Waterfall plots, generated from SHAP values, effectively illustrate how specific characteristics may increase or decrease the risk of particular events for individual patients. Furthermore, the Individual Conditional Expectation approach enables the examination of the specific impact of variable characteristics on

model predictions, allowing clinicians to observe how changes in individual observations affect predicted values. This insight provides a valuable foundation for understanding DL results and facilitating appropriate interventions regarding patients' risk factors. Finally, time-to-event modeling can be employed to proactively reduce the likelihood of adverse events by assessing the probability of specific occurrences over time on an individual level.



## OTHER APPLICATIONS

Improving the quality of MPI images is crucial for enhancing diagnostic efficacy. One of the primary challenges in MPI image quality is soft tissue attenuation, which often results from anatomical structures such as the diaphragm, breast tissue, or obesity.<sup>26,27</sup> These factors can introduce artifacts and distortions that may impede accurate interpretation of the images. To address this issue, tissue AC techniques have been developed to improve the diagnostic accuracy of MPI, and one common AC method is the use of integrated computed tomography (CT) scans. But most cardiac devices do not have integrated CT. Shi et al.<sup>28</sup> developed a deep CNN for AC. DL-based AC images corresponded with CT-based AC images in terms of qualitative and quantitative results. Yang et al.<sup>29</sup> utilized DL for directly performing AC. DL-AC significantly reduces attenuation artifacts compared to CT-AC. Later, Chen et al.<sup>30</sup> further investigated both indirect and direct AC method. The indirect method generates attenuation maps ( $\mu$ -maps) from emission images, while the direct method predicts AC images directly from non-attenuation corrected (NAC) images without  $\mu$ -maps. The results suggested that the indirect method showed superior AC performance than the direct method. More recently, Shanbhag et al.<sup>31</sup> illustrated that the DL-AC TPD and CT-AC TPD had high concordance in IHD diagnosis (AUC 0.79 vs. 0.81). It is notable that the DL-AC effect was not consistent between participants, thus further studies are necessary to improve the stability of the model.

## CHALLENGES AND FUTURE DIRECTIONS FOR DL IN MPI

### Challenges

The accuracy and generalizability of DL models pose challenges to the broader clinical applications of DL in MPI. These challenges arise from several factors, including differences in MPI equipment and acquisition processes across organizations and variations in image quality due to differences in visual and manual interpretation during post-processing quality control. Another challenge lies in the selection of the training population for DL models, which often consists of individuals at high risk of IHD. This biased selection may result in an overestimation of disease prevalence and may not accurately represent the broader population. Furthermore, one of the challenges in the application of DL models is the variability in diagnostic criteria and the selection of adverse cardiovascular prognostic outcomes. The ability to effectively apply DL models to specific clinical situations can be quite challenging. In the future, the development and validation of DL models for diagnostic and prognostic prediction of MPI would greatly benefit from large-scale, multicenter datasets. These datasets would enable a comprehensive assessment of the validity and stability of DL models in different clinical settings.

The generalizability of DL models can be enhanced by collecting a broader range of data through multicenter clinical studies. Additionally, new domain adaptation techniques, such as transfer learning, enable models to adjust effectively to data from different environments. Secondly, the explainability of DL models is critical for clinicians to understand the underlying rationale behind the model's decisions. This can be achieved through explainable tools like SHAP and LIME, as well as by establishing

a transparent model-building process that combines rule-based models with more complex algorithms, making the prediction results easier to comprehend. Regarding clinical integration, the adoption of DL technology can be expedited by training healthcare professionals in AI-related topics, equipping them with the necessary skills to effectively utilize these innovative tools.

### Future directions

With the rapid development of high-information imaging technology, DL-based multi-omics big data have opened up new possibilities for precise analysis. This presents a significant opportunity for transitioning the modern paradigm of precision medicine. In the future, DL technology may jointly analyze MPI images with serological markers and metabolomics markers, enabling the prediction of micro-metabolism from macro-images in cardiovascular diseases. Moreover, it may also combine with bioinformatics databases; it becomes possible to analyze new biomarkers and identify different subtypes of cardiovascular diseases. This connection between basic research and clinical applications in nuclear cardiology allows for a more comprehensive understanding of cardiovascular diseases and their underlying mechanisms. It can also combine with bioinformatics databases to analyze new biomarkers and cardiovascular disease subtypes, connecting basic research and clinical applications in nuclear cardiology. By identifying patients at high risk for CAD at the genetic and metabolic level, we may achieve primary prevention and provide appropriate interventions to reduce the incidence of CAD at its source. Additionally, implementing risk stratification for patients with CAD can facilitate precision medicine by analyzing how patients' responses to mitigating risk factors, such as smoking cessation, and enhancing positive factors, such as increased physical activity, can lower the likelihood of adverse cardiac events. This approach aims to improve patient motivation and allows for real-time adjustments to treatment strategies, ultimately enhancing the quality of life for patients with CAD. Achieving a precise diagnosis and prognostic management of cardiovascular diseases can assist physicians in providing appropriate interventions to reduce the incidence of adverse cardiovascular events.

## CONCLUSION

In conclusion, the application of DL in MPI has demonstrated significant potential in enhancing the efficiency and quality of diagnosis and prognosis, and it mainly includes (1) improving the diagnostic efficacy of myocardial ischemia, (2) providing accurate prognostic predictions for patients with IHD, and (3) increasing image quality such as image AC. With the assistance of DL technology, clinicians can achieve significant economic and health benefits through early diagnosis of CAD, as well as during prognostic assessment, adjustment of treatment strategies, and enhancement of patient outcomes. Physicians should proactively adapt to these changes and approach the results of DL with a cautious attitude and a commitment to continuous learning. They should aim to maximize the benefits of DL technology in improving patient diagnosis and prognosis.

## ACKNOWLEDGMENTS

The study was supported by the Noncommunicable Chronic Diseases-National Science and Technology Major Project (no. 2023ZD0513500) and the National Natural Science Foundation of China (o. 82402317).

## AUTHOR CONTRIBUTIONS

K.S. and F.Y. had the idea for the article; X.H. and H.Z. performed the literature search and initial writing; and Y.H., F.C., Y.L., and J.Z. critically revised the work.

## DECLARATION OF INTERESTS

The authors declare no competing interests.

## REFERENCES

- Mensah, G.A., Fuster, V., Murray, C.J.L., Roth, G.A., Global Burden of Cardiovascular Diseases and Risks Collaborators; Abate, Y.H., Abbasian, M., Abd-Allah, F., Abdollahi, A., Abdollahi, M., and Abdulah, D.M. (2023). Global Burden of Cardiovascular Diseases and Risks, 1990–2022. *J. Am. Coll. Cardiol.* *82*, 2350–2473. <https://doi.org/10.1016/j.jacc.2023.11.007>.
- Montone, R.A., Camilli, M., Calvieri, C., Magnani, G., Bonanni, A., Bhatt, D.L., Rajagopalan, S., Crea, F., and Niccoli, G. (2024). Exosome in Ischaemic Heart Disease: Beyond Traditional Risk Factors. *Eur. Heart J.* *45*, 419–438. <https://doi.org/10.1093/eurheartj/ehae001>.
- Dewey, M., Siebes, M., Kachelrieß, M., Kofoed, K.F., Maurovich-Horvat, P., Nikolaou, K., Bai, W., Kofler, A., Manka, R., Kozerke, S., et al. (2020). Clinical quantitative cardiac imaging for the assessment of myocardial ischaemia. *Nat. Rev. Cardiol.* *17*, 427–450. <https://doi.org/10.1038/s41569-020-0341-8>.
- Hinton, G.E., and Salakhutdinov, R.R. (2006). Reducing the Dimensionality of Data with Neural Networks. *Science* *313*, 504–507. <https://doi.org/10.1126/science.1127647>.
- Esteva, A., Robicquet, A., Ramsundar, B., Kuleshov, V., DePristo, M., Chou, K., Cui, C., Corrado, G., Thrun, S., and Dean, J. (2019). A Guide to Deep Learning in Healthcare. *Nat. Med.* *25*, 24–29. <https://doi.org/10.1038/s41591-018-0316-z>.
- Slomka, P., Xu, Y., Berman, D., and Germano, G. (2012). Quantitative analysis of perfusion studies: strengths and pitfalls. *J. Nucl. Cardiol.* *19*, 338–346. <https://doi.org/10.1007/s12350-011-9509-2>.
- Vasilopoulou, M., Asimakopoulou, Z., Velissari, J., Vicha, A., Rizogianni, M., Pusa, S., Stöven, S., Ficarra, S., Bianco, A., Jiménez-Pavón, D., et al. (2024). Interventions about physical activity and diet and their impact on adolescent and young adult cancer survivors: a Prisma systematic review. *Support Care Cancer* *32*, 342.
- Betancur, J., Commandeur, F., Motlagh, M., Sharir, T., Einstein, A.J., Bokhari, S., Fish, M.B., Ruddy, T.D., Kaufmann, P., Sinusas, A.J., et al. (2018). Deep Learning for Prediction of Obstructive Disease From Fast Myocardial Perfusion SPECT: A Multicenter Study. *JACC. Cardiovasc. Imaging* *11*, 1654–1663. <https://doi.org/10.1016/j.jcmg.2018.01.020>.
- Papandrianos, N.I., Feleki, A., Papageorgiou, E.I., and Martini, C. (2022). Deep Learning-Based Automated Diagnosis for Coronary Artery Disease Using SPECT-MPI Images. *J. Clin. Med.* *11*, 3918. <https://doi.org/10.3390/jcm11133918>.
- Otaki, Y., Singh, A., Kavanagh, P., Miller, R.J.H., Parekh, T., Tamarappoo, B.K., Sharir, T., Einstein, A.J., Fish, M.B., Ruddy, T.D., et al. (2022). Clinical Deployment of Explainable Artificial Intelligence of SPECT for Diagnosis of Coronary Artery Disease. *JACC. Cardiovasc. Imaging* *15*, 1091–1102. <https://doi.org/10.1016/j.jcmg.2021.04.030>.
- Betancur, J., Hu, L.H., Commandeur, F., Sharir, T., Einstein, A.J., Fish, M.B., Ruddy, T.D., Kaufmann, P.A., Sinusas, A.J., Miller, E.J., et al. (2019). Deep Learning Analysis of Upright-Supine High-Efficiency SPECT Myocardial Perfusion Imaging for Prediction of Obstructive Coronary Artery Disease: A Multicenter Study. *J. Nucl. Med.* *60*, 664–670. <https://doi.org/10.2967/jnumed.118.213538>.
- Miller, R.J.H., Kuronuma, K., Singh, A., Otaki, Y., Hayes, S., Chareonthawee, P., Kavanagh, P., Parekh, T., Tamarappoo, B.K., Sharir, T., et al. (2022). Explainable Deep Learning Improves Physician Interpretation of Myocardial Perfusion Imaging. *J. Nucl. Med.* *63*, 1768–1774. <https://doi.org/10.2967/jnumed.121.263686>.
- Liu, H., Wu, J., Miller, E.J., Liu, C., Yaqiang, L., and Liu, Y.H. (2021). Diagnostic Accuracy of Stress-Only Myocardial Perfusion SPECT Improved by Deep Learning. *Eur. J. Nucl. Med. Mol. Imaging* *48*, 2793–2800. <https://doi.org/10.1007/s00259-021-05202-9>.
- Kaplan Berkaya, S., Ak Sivriköz, I., and Gunal, S. (2020). Classification Models for SPECT Myocardial Perfusion Imaging. *Comput. Biol. Med.* *123*, 103893. <https://doi.org/10.1016/j.compbiomed.2020.103893>.
- Teuhu, J., Schultz, J., Klén, R., Juárez-Orozco, L.E., Knuuti, J., Saraste, A., Ono, N., and Kanaya, S. (2024). Explainable deep-learning-based ischemia detection using hybrid O-15 H<sub>2</sub>O perfusion positron emission tomography and computed tomography imaging with clinical data. *J. Nucl. Cardiol.* *8*, 101889.
- Kusumoto, D., Akiyama, T., Hashimoto, M., Iwabuchi, Y., Katsuki, T., Kimura, M., Akiba, Y., Sawada, H., Inohara, T., Yuasa, S., et al. (2024). A deep learning-based automated diagnosis system for SPECT myocardial perfusion imaging. *Sci. Rep.* *14*, 13583.
- Regitz-Zagrosek, V., and Gebhard, C. (2023). Gender Medicine: Effects of Sex and Gender on Cardiovascular Disease Manifestation and Outcomes. *Nat. Rev. Cardiol.* *20*, 236–247. <https://doi.org/10.1038/s41569-022-00797-4>.
- Zhang, H., Caobelli, F., Che, W., Huang, Y., Zhang, Y., Fan, X., Hu, X., Xu, C., Fei, M., Zhang, J., et al. (2023). The Prognostic Value of CZT SPECT Myocardial Blood Flow (MBF) Quantification in Patients with Ischemia and No Obstructive Coronary Artery Disease (INOCA): A Pilot Study. *Eur. J. Nucl. Med. Mol. Imaging* *50*, 1940–1953. <https://doi.org/10.1007/s00259-023-06125-3>.
- Wang, J., Fan, X., Qin, S., Shi, K., Zhang, H., and Yu, F. (2022). Exploration of the Efficacy of Radiomics Applied to Left Ventricular Tomograms Obtained from D-SPECT MPI for the Auxiliary Diagnosis of Myocardial Ischemia in CAD. *Int. J. Cardiovasc. Imaging* *38*, 465–472. <https://doi.org/10.1007/s10554-021-02413-x>.
- Miller, R.J.H., Singh, A., Otaki, Y., Tamarappoo, B.K., Kavanagh, P., Parekh, T., Hu, L.H., Gransar, H., Sharir, T., Einstein, A.J., et al. (2023). Mitigating Bias in Deep Learning for Diagnosis of Coronary Artery Disease from Myocardial Perfusion SPECT Images. *Eur. J. Nucl. Med. Mol. Imaging* *50*, 387–397. <https://doi.org/10.1007/s00259-022-05972-w>.
- Kopeva, K.V., Mochula, A.V., Maltseva, A.N., Soldenko, M.V., Grakova, E.V., and Zavadovsky, K.V. (2023). Prognostic Role of Dynamic CZT Imaging in Heart Failure With Preserved Ejection Fraction. *Clin. Nucl. Med.* *48*, e364–e370. <https://doi.org/10.1097/RLU.0000000000004738>.
- Miller, R.J.H., Shanbhag, A., Killekar, A., Lemley, M., Bednarski, B., Van Kriekinge, S.D., Kavanagh, P.B., Feher, A., Miller, E.J., Einstein, A.J., et al. (2024). AI-derived epicardial fat measurements improve cardiovascular risk prediction from myocardial perfusion imaging. *NPJ Digit. Med.* *7*, 24.
- Miller, R.J.H., Hu, L.H., Gransar, H., Betancur, J., Eisenberg, E., Otaki, Y., Sharir, T., Fish, M.B., Ruddy, T.D., Dorbala, S., et al. (2020). Transient Ischaemic Dilation and Post-Stress Wall Motion Abnormality Increase Risk in Patients with Less than Moderate Ischaemia: Analysis of the REFINE SPECT Registry. *Eur. Heart J. Cardiovasc. Imaging* *21*, 567–575. <https://doi.org/10.1093/ehjci/jez172>.
- Singh, A., Miller, R.J.H., Otaki, Y., Kavanagh, P., Hauser, M.T., Tzolos, E., Kwiecinski, J., Van Kriekinge, S., Wei, C.C., Sharir, T., et al. (2023). Direct Risk Assessment From Myocardial Perfusion Imaging Using Explainable Deep Learning. *JACC. Cardiovasc. Imaging* *16*, 209–220. <https://doi.org/10.1016/j.jcmg.2022.07.017>.

25. Pieszko, K., Shanbhag, A.D., Singh, A., Hauser, M.T., Miller, R.J.H., Liang, J.X., Motwani, M., Kwiecieński, J., Sharir, T., Einstein, A.J., et al. (2023). Time and Event-Specific Deep Learning for Personalized Risk Assessment after Cardiac Perfusion Imaging. *NPJ Digit. Med.* 6, 78. <https://doi.org/10.1038/s41746-023-00806-x>.
26. Rahman, M.A., Yu, Z., Laforest, R., Abbey, C.K., Siegel, B.A., and Jha, A.K. (2024). DEMIST: A Deep-Learning-Based Detection-Task-Specific Denoising Approach for Myocardial Perfusion SPECT. *IEEE Trans. Radiat. Plasma Med. Sci.* 8, 439–450.
27. Torkaman, M., Yang, J., Shi, L., Wang, R., Miller, E.J., Sinusas, A.J., Liu, C., Gullberg, G.T., and Seo, Y. (2022). Data Management and Network Architecture Effect on Performance Variability in Direct Attenuation Correction via Deep Learning for Cardiac SPECT: A Feasibility Study. *IEEE Trans. Radiat. Plasma Med. Sci.* 6, 755–765.
28. Shi, L., Onofrey, J.A., Liu, H., Liu, Y.H., and Liu, C. (2020). Deep Learning-Based Attenuation Map Generation for Myocardial Perfusion SPECT. *Eur. J. Nucl. Med. Mol. Imaging* 47, 2383–2395. <https://doi.org/10.1007/s00259-020-04746-6>.
29. Yang, J., Shi, L., Wang, R., Miller, E.J., Sinusas, A.J., Liu, C., Gullberg, G.T., and Seo, Y. (2021). Direct Attenuation Correction Using Deep Learning for Cardiac SPECT: A Feasibility Study. *J. Nucl. Med.* 62, 1645–1652. <https://doi.org/10.2967/jnumed.120.256396>.
30. Chen, X., Zhou, B., Xie, H., Shi, L., Liu, H., Holler, W., Lin, M., Liu, Y.H., Miller, E.J., Sinusas, A.J., and Liu, C. (2022). Direct and Indirect Strategies of Deep-Learning-Based Attenuation Correction for General Purpose and Dedicated Cardiac SPECT. *Eur. J. Nucl. Med. Mol. Imaging* 49, 3046–3060. <https://doi.org/10.1007/s00259-022-05718-8>.
31. Shanbhag, A.D., Miller, R.J.H., Pieszko, K., Lemley, M., Kavanagh, P., Feher, A., Miller, E.J., Sinusas, A.J., Kaufmann, P.A., Han, D., et al. (2023). Deep Learning-Based Attenuation Correction Improves Diagnostic Accuracy of Cardiac SPECT. *J. Nucl. Med.* 64, 472–478. <https://doi.org/10.2967/jnumed.122.264429>.